

Applications of false-coloring of black and white imagery  
by Optical Density Encoding Techniques

Hu Ruiming; Yang Suqin"

---

ABSTRACT

This paper presents the principle of the Optical Density Encoding Technique(ODET) for false-coloring of b/w imagery(BWI) in three steps. A new white-light ZOOM processor(WLZP) is designed and used instead of 4f system. The false-color imagery(FCI) with different enlargement can be directly obtained in the WLZP. It is cheap in cost, efficient and convenient in operation and smaller in space. The advantages of the ODET are discussed. The interpretational analyses of the processing results are reported.

---

Introduction

Each band of the BWI from Multispectral Scanner Landsat Data, the aerial BWI and various BWI contain huge information. The pity is that only ten and more b/w grey tones can be distinguished by the human eye. However, it can distinguish more than one hundred colors in whole spectrum. Therefore, to transform each single b/w imagery with small grey differences into FCI according to their grey tones can fully extract the information contained and can enhance the resolving power of the human eye enormously. This is the false-coloring effect of the ODET. Investigation of various image processing techniques(IPT) to enhance the interpretational effect of the BWI has become an extremely active field.<sup>(2-6)</sup>

Most of the IPTs are digital so far. However, there are three main disadvantages in digital IPT: high cost; complicated processing techniques and limited resolution by the sample points.

This paper presents an approach of the ODET which is one of the IPTs. There are some obvious advantages in this approach compared with the digital IPT:

low cost; easier processing techniques; high speed; huge capacity; high sensitivity to small density differences and almost continuous transition of the colors. Only one single BWI is needed in this approach, although multiple bands superimposition is possible.<sup>1</sup> However, single band processing is simple and can extract the information contained in each single band in more detail separately.

Basic principle and approach

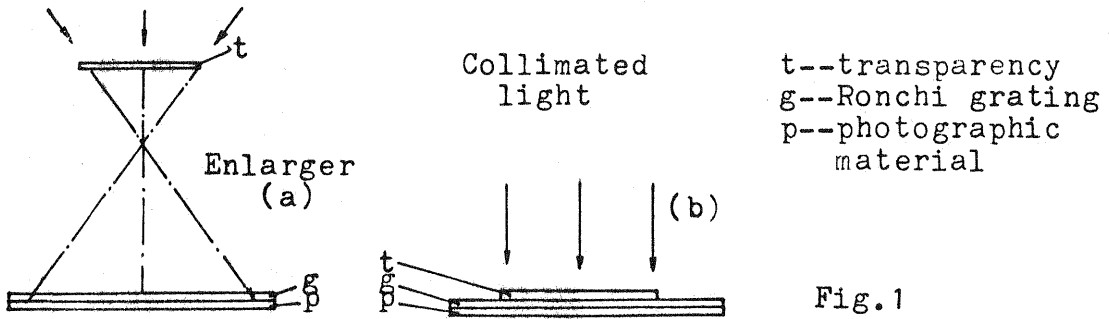
The basic principle of this approach is to use the optical diffraction effect of a phase grating modulated by the BWI in a white-light optical processor. The phase function in the phase grating is proportional to the density function in the BWI. The FCI can be obtained by means of filtering in the spectral plane of the processor. The principle will be explained in three steps:

(1) Encoding of the BWI

---

<sup>1</sup>, "College of Engineering, Univ. of Hainan, Hainan Island, China

Usually, the Ronchi Grating is used to encode the BWI. There are basically two methods for encoding. The one is using an enlarger and the other is using the collimated light beam as in Fig.1:

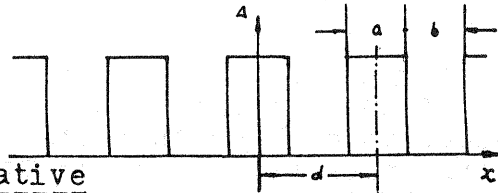


A negative of the encoded BWI can be obtained, if the exposure, developing and fixing of the negative are processed properly. The transmissivity function of the encoded negative can be written as:

$$T(x) = t(x) + t_1(x) e^{i \frac{2\pi}{\lambda} \Delta} \quad (1)$$

where  $t(x) = \text{rect}\left(\frac{x}{a}\right) - \frac{1}{d} \text{comb}\left(\frac{x}{d}\right)$ ,  $t_1(x) = \text{rect}\left(\frac{x}{b}\right) - \frac{1}{d} \text{comb}\left(\frac{x+d}{d}\right)$

Fig.2



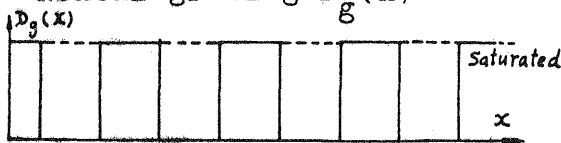
(2) Bleaching of the encoded negative

Having bleached the encoded negative, a transparent phase grating (TPG) modulated by the BWI is obtained. The relief function of the TPG is the same as that of the encoded negative and is proportional to the density function of the BWI. Let the width of the phase grating be  $c$ . When the monochromatic light is used, the  $T(x)$  transmissivity function of the TPG can be written as:

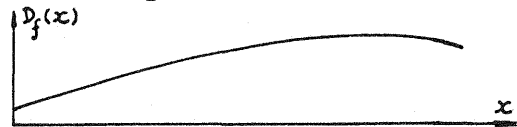
$$T(x) = \left( \left( \text{rect}\left(\frac{x}{a}\right) - \frac{1}{d} \text{comb}\left(\frac{x}{d}\right) \right) + \left( \text{rect}\left(\frac{x}{b}\right) - \frac{1}{d} \text{comb}\left(\frac{x+d}{d}\right) \cdot e^{i \frac{2\pi}{\lambda} \Delta} \right) \right) \cdot \text{rect}\left(\frac{x}{c}\right) \quad (2)$$

The procedures for making a TPG can be depicted as follows:

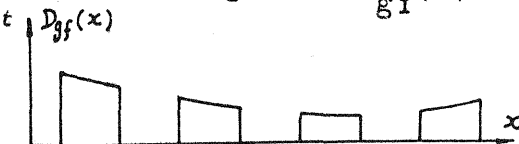
1) Density function of the Ronchi grating  $D_g(x)$



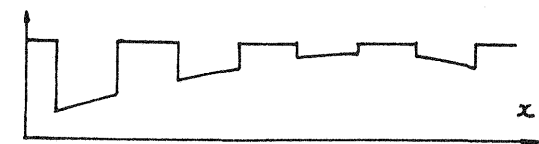
2) Density function of the BWI  $D_f(x)$



3) Density function of the encoded negative  $D_{gf}(x)$



4) Transmissivity function of the TPG  $t(x)$



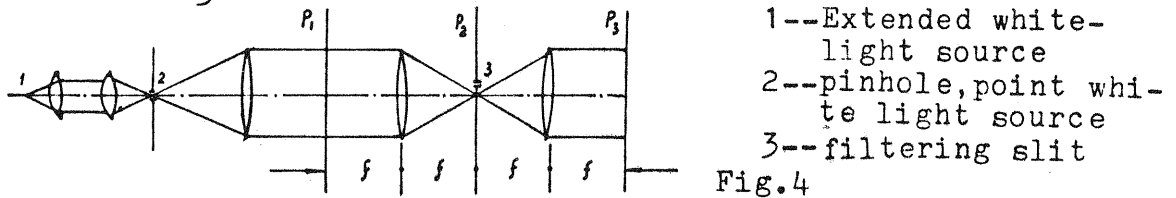
5) Phase function of the TPG  $\varphi(x)$



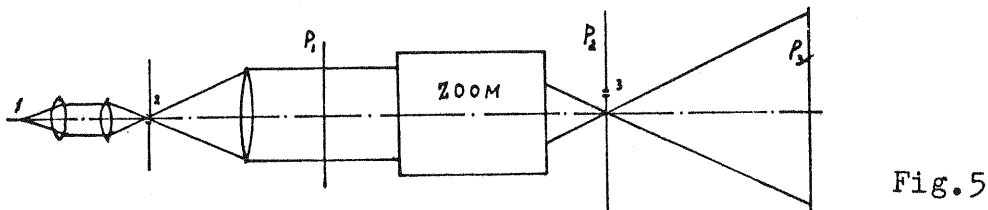
Fig.3

(3) Decoding of the TPG by means of filtering in the spectral plane of the white-light optical processor(WLCP)

The TPG bleached is put in the input plane  $P_1$ ,  $P_2$  is the spectral plane and  $P_3$  is the output plane of the WLOP as shown in Fig.4



This is a standard 4f system of the WLOP. However, it is difficult to get the enlarged FCI directly. In this paper, a new WLOP with a simple ZOOM is designed and used for false-coloring. We call it the white-light ZOOM processor(WLZM) as shown in Fig.5.



The enlarged FCI can be directly obtained in the WLZM, the enlargement of the FCI can be adjusted by the ZOOM easily and the space needed is smaller than other designs. (4)

The transmissivity function  $T(\xi)$  in  $P_2$  is the Fourier transform of the  $T(x)$  in  $P_1$ :

$$T(\xi) = \mathcal{F}(T(x)) \quad (3)$$

The filtering is done in the spectral plane  $P_2$  of the WLZM by means of a slit, through it only one order of the spectrum can be passed. The transmissivity function of the complex amplitude function in  $P_3$  is the inverse Fourier transform of the  $T(\xi)$  in  $P_2$ . The intensity function in the output plane  $P_3$  can be written as:

$$\begin{aligned} I_n(\Delta, \lambda) &= \mathcal{F}^{-1}(T_n(\xi)) \cdot \mathcal{F}^{-1}(T_n^*(\xi)) \\ &= I(\lambda) \left( \left( \frac{a}{d} \text{Sinc}\left(\frac{na}{d}\right) \right)^2 + \left( \frac{b}{d} \text{Sinc}\left(\frac{nb}{d}\right) \right)^2 + \frac{2ab}{d^2} \text{Sinc}\left(\frac{na}{d}\right) \text{Sinc}\left(\frac{nb}{d}\right) \right. \\ &\quad \left. \cos\left(n\pi + \frac{2\pi}{\lambda} \Delta\right) \right) \end{aligned} \quad (4)$$

$$\left. \begin{aligned} \text{Let } A_n &= \left( \frac{a}{d} \text{Sinc}\left(\frac{na}{d}\right) \right)^2 + \left( \frac{b}{d} \text{Sinc}\left(\frac{nb}{d}\right) \right)^2 \\ B_n &= 2 \frac{ab}{d^2} \text{Sinc}\left(\frac{na}{d}\right) \text{Sinc}\left(\frac{nb}{d}\right) \end{aligned} \right\}, \text{ then}$$

$$I_n(\Delta, \lambda) = I(\lambda) \left( A_n + B_n \cos\left(\frac{2\pi}{\lambda} \Delta + n\pi\right) \right) \quad (5)$$

If  $a=b=\frac{d}{2}$ , then  $A_n = B_n = \frac{1}{2} \text{Sinc}^2\left(\frac{n}{2}\right)$ . For white-light, we have

$$I_n(\Delta, \lambda) = \int I(\lambda) \left( A_n + B_n \cos\left(\frac{2\pi}{\lambda} \Delta + n\pi\right) d\lambda \right) \quad (6)$$

It is thus obvious that the intensity function  $I_n(\Delta, \lambda)$  in the  $P_3$  is the result of incoherent overlapping with the light of different wave lengths and weights.

After integration, we have

$$I_n(\Delta, \lambda) = \sum_{\lambda} \frac{I(\lambda)}{2} \text{Sinc}^2\left(\frac{n}{2}\right) \cdot (1 + \text{Cos}\left(\frac{2n\Delta}{\lambda} + n\pi\right)) \quad (7)$$

For the zero order of the spectrum,  $n=0$  and let  $I(\lambda)=1$ , then

$$I_0(\Delta, \lambda) = \sum_{\lambda} \frac{1}{2} (1 + \text{Cos}\left(\frac{2\pi\Delta}{\lambda}\right)) \quad (8)$$

For the first order, we have

$$I_1(\Delta, \lambda) = \sum_{\lambda} \frac{2}{\pi^2} (1 - \text{Cos}\left(\frac{2\pi\Delta}{\lambda}\right)) \quad (9)$$

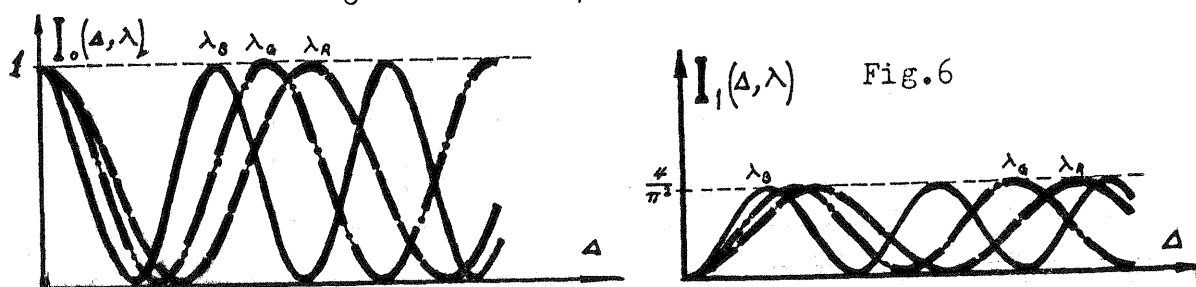
For the odd order, we have

$$I_{\text{odd}}(\Delta, \lambda) = \sum_{\lambda} \frac{2}{n^2\pi^2} (1 - \text{Cos}\left(\frac{2\pi\Delta}{\lambda}\right)) \quad (10)$$

For the even order, we have

$$I_{\text{even}}(\Delta, \lambda) = 0 \quad (11)$$

We can show how the false-colors are composed of three primary colors for  $I_0(\Delta, \lambda)$  and  $I_1(\Delta, \lambda)$  as follows:



Usually, the lower order of the spectrum is selected in filtering. Therefore, the high utilization ratio of the light energy can be expected. From the equation (8) and (9), it is clear that the different color effects can be obtained by the order selection in filtering, e.g., complementary FCI can be obtained by interchanging the zero and first order of the spectrum in filtering.

### Report on applications

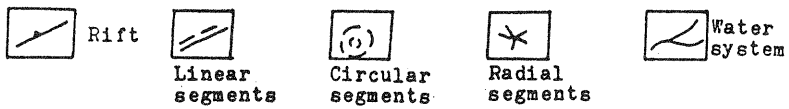
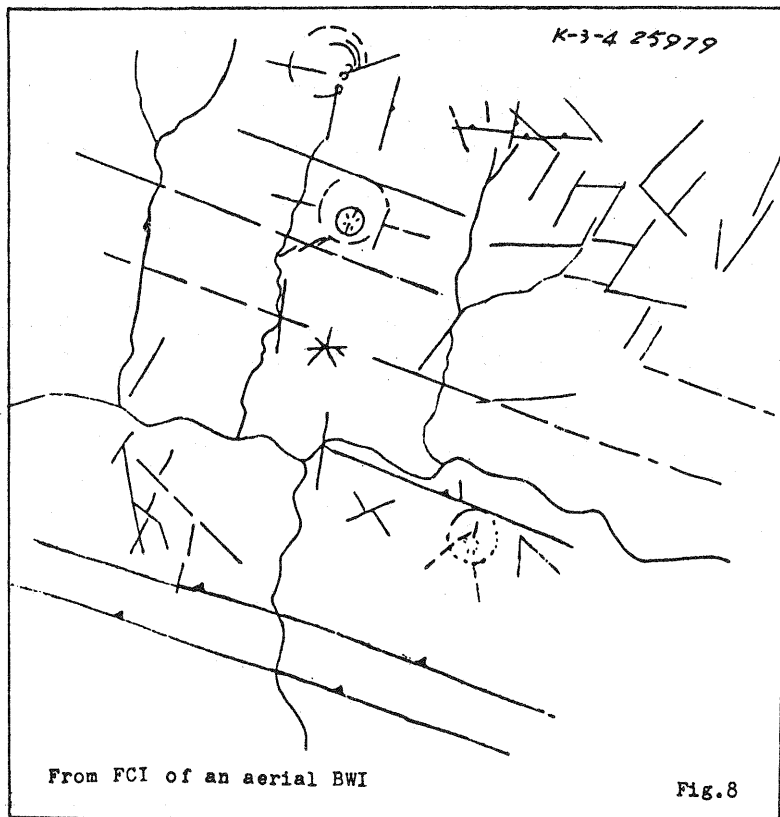
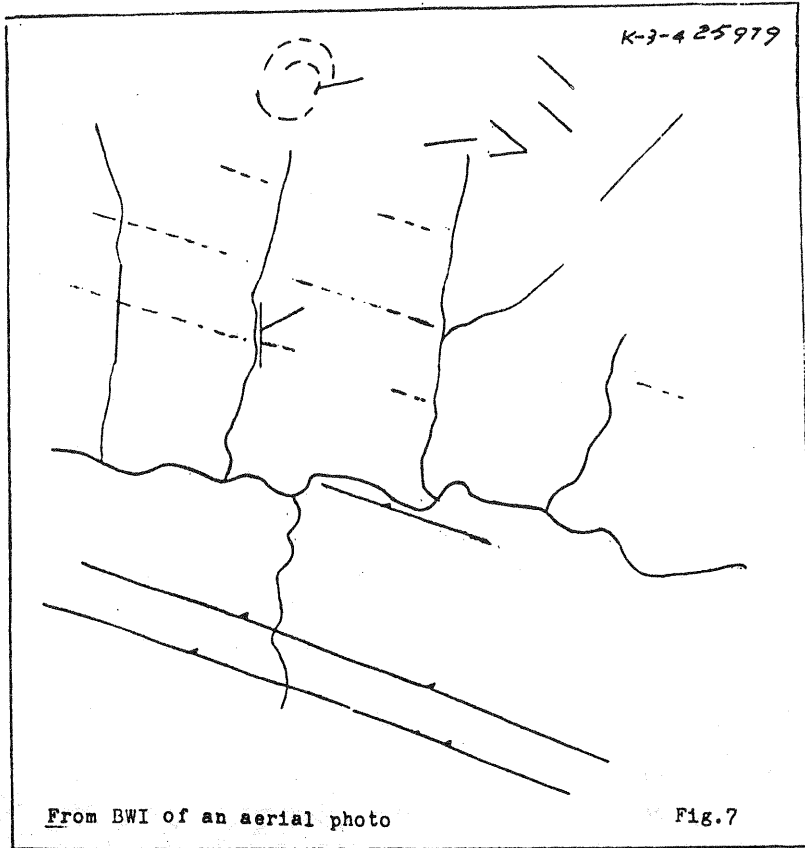
Various FCI of the BWI have been made by the WLZP mentioned above for interpretational analyses. The results center on two themes with five sample FCI.

#### Applications for revealing the geological structural features.

Two sample FCI are presented for this applications.

(1) the FCI of an aerial BWI, format 23 cm×23 cm, of Qin Mountains, Shanxi Province, China.

According to the existing geological map of scale 1:200,000, the lineaments on this aerial photo are the strata of the middle Devonian, and the lithology belongs to the clastic rock. Interpretability of the FCI is enhanced. Ten and more linear segments which are bigger than 0.5mm have been revealed. Some of them can be directly determined as the fractural structures and the intersection relationships are clear. In addition, two more indistinct circular traces and one more radial structure have been revealed. ( see Fig.7,8 and corresponding BWI and FCI )



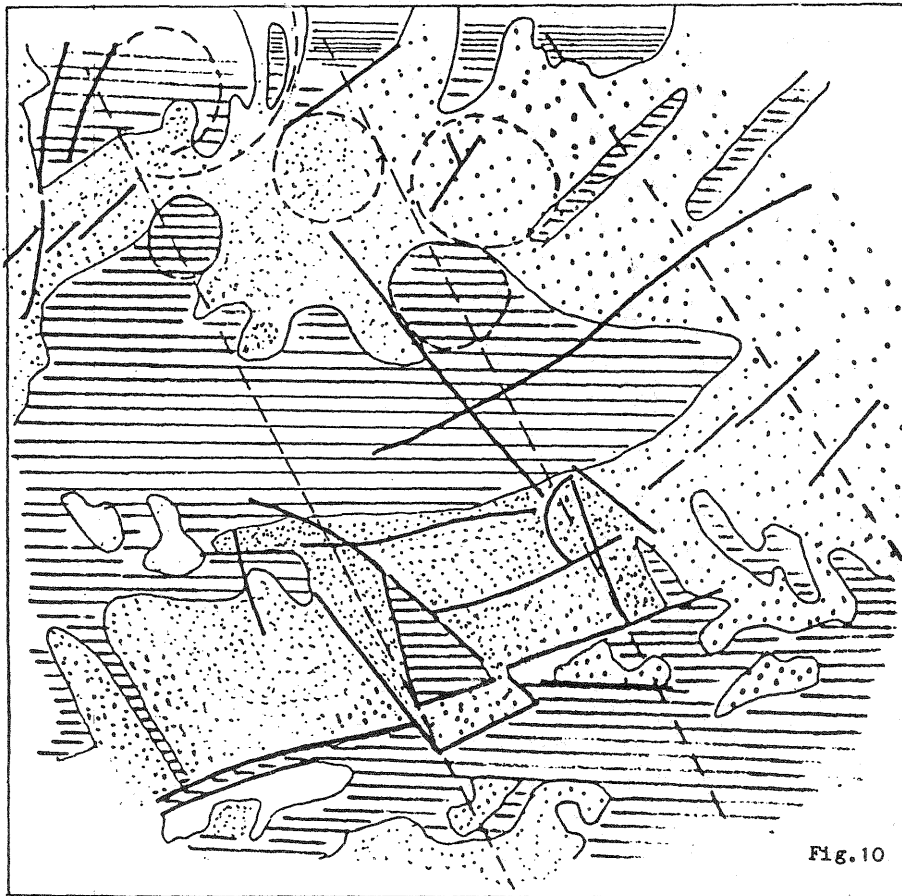
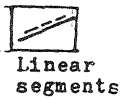


Fig. 10

From FCI of MSS 7



Linear segments



Circular segment



Outcropping bedrock



Broken and sunken basin



Boundaries with different colors in NNW direction

ERTS-2 MSS7

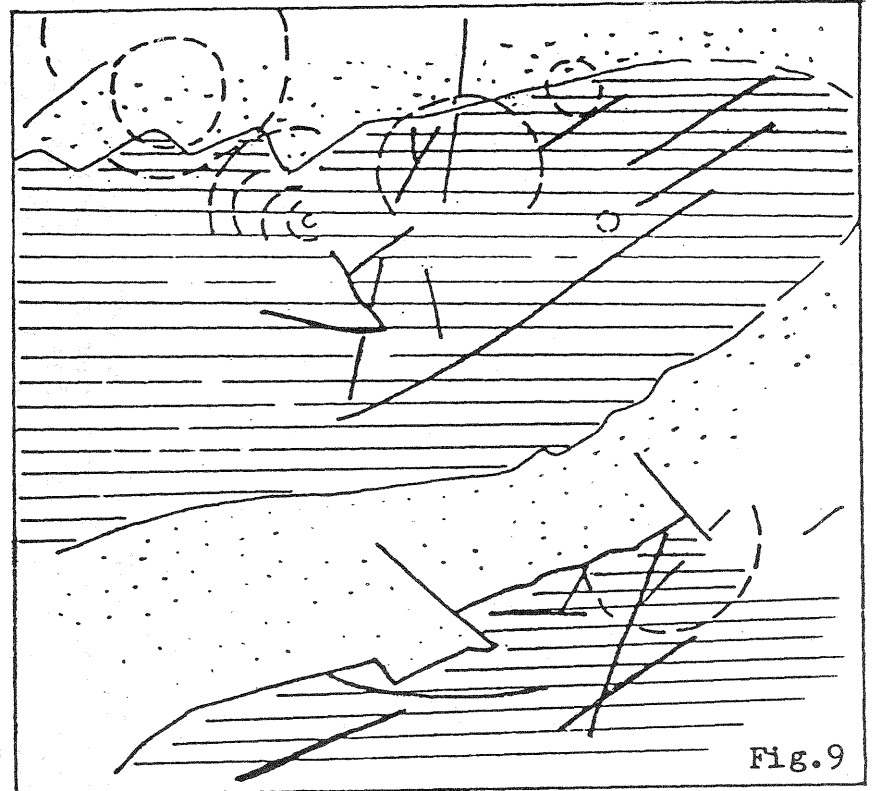


Fig. 9

From BWI of MSS 7

ERTS-2 MSS7



Linear segments



Circular segment



Outcropping bedrock



Broken and sunken basin

It is clearly shown on the FCI that the stratigraphical strike is in NNW direction.

(2) The FCI of a band 7 of the MSS Landsat Data dated May 11, 1975 (format 70mm×70mm) covered the Altai region in Xinjiang Province, China.

In this FCI, the outcrops of the bedrock are revealed more in detail, circular traces and circles composed of different colors represent basically the outcrops of the granite. The centers of the circles may be the centers of the magma activities. In addition, the boundaries with different colors along the NNW direction can be clearly seen. This may represent the phenomenon of the old basal structure. Having compared with the geological data, we have found that some superbedrocks are revealed intermittently along the boundaries of the rose and light green areas. Aeromagnetic anomaly had the tendency to spread along the NNW direction as well. ( see Fig.9,10 and corresponding BWI and FCI )

#### Applications for revealing the subsurface geological structures

Two sample FCI are presented in this applications. One of them is the same as the previous one.

(1) The same FCI as the previous one

Some parts of the Altai regions were covered by sand and snow. In this FCI processed, the linear segments are clearly visible in the broken and sunken basin. These segments can be interpreted as the subsurface rifts. It is impossible to recognize and identify them by the ordinary field methods. This represents that the FCI has the so-called "penetration effect".

(2) The FCI of a band 7 of the MSS Landsat Data (format 70mm×70mm) of the Erlian Haote region in Inner Mongolia Autonomous Region.

The west part of the Xilamolun River rift is situated in this FCI according to the existing data. This area has been covered by the loose sedimentary succession. Some outcrops of the Palaeozoic strata have been intermingled. These and the Cenozoic strata have formed the Inner Mongolia Plateau. On this Plateau, the terrain is smooth, the landform is indistinct, the contrast of the images is quite low and the traces of the rifts are not clear. Traces of the rifts are not clear in the FCI by the digital IPTs.

The FCI processed by the WLZP displays a linear trace of the rift clearly with different colors. Therefore, the WLZP can be recommended to be a new auxiliary means for the interpretation analyses of the subsurface fractural structures in investigation of mineralogy and seismology.

#### Applications in investigation of agricultural resources

Two sample FCI are presented in this applications.

(1) Two FCI of MSS Landsat Data of the Wuhan region in Hubei Province, China, format 70mm×70mm, band 7 and 4.

The sample area which is mountainous is in the right lower corner of the Wuhan region. The contrast of this area is so high that it is difficult or even unable to distinguish the coniferous or broad leaf forests, grass or bushes in the BWI. When an incoherent false-color composite equipment is used, the colors ob-

tained all belong to a series of red color tones. Therefore, the color differences are not obvious and it is difficult to interpret with such a FCI. However, the ODET is used for false-coloring, the different categories of the agricultural resources are displayed by the different false-colors. Then it is much easier to interpret with such a FCI. In the FCI of band 7, the coniferous trees are bright red, broad leaf trees and bamboo forests are dark blue, grasses and bushes are yellow-green, double harvest rice in the basin of the mountainous areas present blue-green, single harvest rice in the ridge of the gullies are pink. However, there are some confusion colors in this FCI of band 7, such as the single harvest rice in the ridges, the brooks and the streams in the mountainous areas are all pink; reservoirs, lakes, the broad leaf trees and bamboo forests are all dark blue. Some of these confusion can be easily distinguished by the shapes and some other known data. In addition, the other bands can be used for false-coloring as well. The band 4 is selected for false-coloring according to the surface reflection spectrum on the ground. The FCI of band 4 shows that the water systems are light yellow, the single harvest rice is pink and the double harvest rice are bright green. By comparing these two FCI, the previous confusion can be probably solved. The result shows that the accuracy of the classification with this approach can almost reach the accuracy level of the digital IPT.

### Conclusion

The FCI obtained with the WLZP of the ODET have many advantages, such as color tones are saturated, bright and abundant; high sensitivity to density differences makes that the linear and circular segments of the surface and subsurface geological structures can be clearly displayed with different colors, therefore, the subsurface fractures and rifts can be revealed; the agricultural resources can be distinguished by the obviously different colors. According to the surface reflection spectrum on the ground to select one more band for false-coloring, the classification accuracy level of digital IPT can be reached.

The ODET comparing with the digital IPT is a new economic, fast and effective means for the investigation of the surface and subsurface geological structures, the mineral resources, seismological geology, the agricultural resources and any other sciences where the BWI information are used. We have processed many other FCI in Medicine such as Ultrasonic BWI, BWI of CT, OM, SEM and TEM which will be reported later in another time.

### REFERENCES

- [1] F.T.S.Yu: Generating False-color composites with a white-light optical processor. PE&RS, 1986, No. 3, (367-371)
- [2] Pons et al: Optical Pseudocoloring Technique to Improve Directional Information, J. Optics (Paris), Vol. 15, No. 2, 1984 (65-67)
- [3] Prieto, A et al: Spatial Frequency Pseudocolor Filters, PE&RS, Vol. 48, No. 11, 1982
- [4] Santamaria, J et al: J. Opt., Vol. 10, No. 15, 1979
- [5] Tai, A et al: Opt. Lett, 3, 190, 1978
- [6] Guo, Lurong et al: Phase False-coloring Modulated by Density Encoding, Journal of Optics, Vol. 4, No. 2, 1984, Academia Sinica